

Chaos driven fusion enhancement factor at astrophysical energies

Sachie Kimura and Aldo Bonasera

Laboratorio Nazionale del Sud, INFN, via Santa Sofia, 62, 95123 Catania, Italy

(Dated: July 8, 2018)

We perform molecular dynamics simulations of screening by bound target electrons in low energy nuclear reactions. Quantum effects corresponding to the Pauli and Heisenberg principle are enforced by constraints. We show that the enhancement of the average cross section and of its variance is due to the perturbations induced by the electrons. This gives a correlation between the maximum amplitudes of the inter-nuclear oscillational motion and the enhancement factor. It suggests that the chaotic behavior of the electronic motion affects the magnitude of the enhancement factor.

PACS numbers: 25.45.-z, 34.10.+x

The knowledge of the bare nuclear reaction rates at low energies is essential not only for the understanding of various astrophysical nuclear problems, but also for assessing the effects of the host materials in low energy nuclear fusion reactions in matter. This is currently a subject of great interest in nuclear physics, since Muenster group has reported that the experimental cross sections of the ${}^3\text{He}(\text{d},\text{p}){}^4\text{He}$ and of ${}^2\text{H}({}^3\text{He},\text{p}){}^4\text{He}$ reactions with gas targets show an increasing enhancement with decreasing bombarding energy with respect to the values obtained by extrapolating from the data at high energies [1]. Many studies attempted to attribute the enhancement of the reaction rate to the screening effects by bound target electrons. In this context one often estimates the screening potential as a constant decrease of the barrier height in the tunneling region through a fit to the data. A puzzle has been that the screening potential obtained by this procedure exceeds the value of the so called adiabatic limit, which is given by the difference of the binding energies of the united atoms and of the target atom and it is theoretically thought to provide the maximum screening potential [2]. Over these several years, the redetermination of the bare cross sections has been proposed theoretically [3] and experimentally [4], using the Trojan Horse Method [5]. The comparison between newly obtained bare cross sections, i.e., astrophysical S-factors, and the cross sections by the direct measurements gives a variety of values for the screening potential. There are already some theoretical studies performed using the time-dependent Hartree-Fock(TDHF) scheme [6, 7].

In this letter we examine the subject within the constrained molecular dynamics (CoMD) model [8], even in the very low incident energy region not reached experimentally yet. At such very low energies fluctuations are anticipated to play a substantial role. Such fluctuations are beyond the TDHF scheme. Not only TDHF calculations are, by construction, cylindrically symmetric around the beam axis. Such a limitation is not necessarily true in nature and the mean field dynamics could be not correct especially in presence of large fluctuations. Molecular dynamics contains all possible correlations and fluctuations due to the initial conditions(events). For the purpose of treating quantum-mechanical systems like tar-

get atoms and molecules, we use classical equations of motion with constraints to satisfy the Heisenberg uncertainty principle and the Pauli exclusion principle for each event [8]. In extending the study to the lower incident energies, we would like to stress the connection between the motion of bound electrons and chaos. In fact, depending on the dynamics, the behavior of the electron(s) is unstable and influence the relative motion of the projectile and the target. We could compare the D+d case to the gravitational 3-body problem, which has the same form of the equation of motion and it is nonintegrable [9]. For instance, the motion of asteroids around the sun perturbed by Jupiter becomes unstable, i.e., chaotic, depending on the ratio of the unperturbed frequencies of the asteroid and Jupiter. We discuss the enhancement factor of the laboratory cross section in connection with the integrability of the system by looking the inter-nuclear and electronic oscillational motion. More specifically we analyze the frequency shift of the target electron due to the projectile and the small oscillational motion induced by the electron to the relative motion between the target and the projectile. We show that the increase of chaoticity in the electron motion decreases the fusion probability. In this letter we will discuss the D+d case only because the system is fundamental to see its connection with chaos and has been well studied theoretically. We mention that the understanding of the fusion dynamics and fluctuations has a great potential for the enhancement of the fusion probability in plasmas for energy production.

We denote the reaction cross section at incident energy in the center of mass E by $\sigma(E)$ and the cross section obtained in absence of electrons by $\sigma_0(E)$. The enhancement factor f_e is defined as

$$f_e \equiv \frac{\sigma(E)}{\sigma_0(E)}. \quad (1)$$

If the effect of the electrons is well represented by the constant shift U_e of the potential barrier, following [6, 10], ($U_e \ll E$):

$$f_e \sim \exp \left[\pi \eta(E) \frac{U_e}{E} \right], \quad (2)$$

where $\eta(E)$ is the Sommerfeld parameter [11].

We estimate the enhancement factor f_e numerically using molecular dynamics approach;

$$\frac{d\mathbf{r}_i}{dt} = \frac{\mathbf{p}_i}{\mathcal{E}_i}, \quad \frac{d\mathbf{p}_i}{dt} = -\nabla_{\mathbf{r}} U(\mathbf{r}_i), \quad (3)$$

where $(\mathbf{r}_i, \mathbf{p}_i)$ are the position, momentum of the particle i at time t . $\mathcal{E}_i = \sqrt{\mathbf{p}_i^2 c^2 + m_i^2 c^4}$, $U(\mathbf{r}_i)$ and m_i are its energy, Coulomb potential and mass, respectively. We set the starting point of the reaction at 10\AA internuclear separation. Initially the electron is located in a Bohr orbit. To take into account the quantum mechanical feature of atoms, we put the constraints, i.e., Heisenberg uncertainty principle and Pauli principle for atoms which have more than 2 bound electrons. It is performed numerically by checking $\Delta\mathbf{r} \cdot \Delta\mathbf{p} \sim \hbar$, for Heisenberg principle, and $\Delta\mathbf{r} \cdot \Delta\mathbf{p} \sim 2\pi\hbar(3/4\pi)^{2/3}$, for Pauli blocking. Here $\Delta\mathbf{r} = |\mathbf{r}_i - \mathbf{r}_j|$ and $\Delta\mathbf{p} = |\mathbf{p}_i - \mathbf{p}_j|$. i and j refer to electrons and nuclei. More specifically, to get the atomic ground states, at every time step of the calculation, we calculate $\Delta\mathbf{r} \cdot \Delta\mathbf{p}$ for every pair of particles. If $\Delta\mathbf{r} \cdot \Delta\mathbf{p}$ is smaller (larger) than \hbar , in the case of Heisenberg principle, we change \mathbf{r}_j and \mathbf{p}_j slightly, so that $\Delta\mathbf{r} \cdot \Delta\mathbf{p}$ becomes larger (smaller) at the subsequent time step. We repeat this procedure for many time steps until no changes are seen in the energies and mean square radii of the atoms, similarly for the Pauli principle. The approach has been successfully applied to treat fermionic properties of the nucleons in nuclei and the quark system [8]. It can be extended easily in the case of the Heisenberg principle, as stated above. In this way we obtain many initial conditions which occupy different points in the phase space microscopically. Notice that in the D+d case that we investigate here, since one electron is involved, only the Heisenberg principle is enforced for each event. We obtain -13.56 eV as the binding energy of deuterium atom and 0.5327 Å as its mean square radius. These values can be compared with the experimental value of -13.59811 eV [12] and Bohr radius $R_B = 0.529$ Å, respectively [13].

In order to treat the tunneling process, we define the collective coordinates \mathbf{R}^{coll} and the collective momentum \mathbf{P}^{coll} as

$$\mathbf{R}^{coll} \equiv \mathbf{r}_P - \mathbf{r}_T; \quad \mathbf{P}^{coll} \equiv \mathbf{p}_P - \mathbf{p}_T, \quad (4)$$

where $\mathbf{r}_T, \mathbf{r}_P$ ($\mathbf{p}_T, \mathbf{p}_P$) are the coordinates (momenta) of the target and the projectile nuclei, respectively. When the collective momentum becomes zero, we switch on the collective force, which is determined by $\mathbf{F}_P^{coll} \equiv \dot{\mathbf{P}}^{coll}$ and $\mathbf{F}_T^{coll} \equiv -\dot{\mathbf{P}}^{coll}$, to enter into imaginary time [14]. We follow the time evolution in the tunneling region using the equations,

$$\frac{d\mathbf{r}_{T(P)}^{\Im}}{d\tau} = \frac{\mathbf{p}_{T(P)}^{\Im}}{\mathcal{E}_{T(P)}}; \quad \frac{d\mathbf{p}_{T(P)}^{\Im}}{d\tau} = -\nabla_{\mathbf{r}} U(\mathbf{r}_{T(P)}^{\Im}) - 2\mathbf{F}_{T(P)}^{coll}, \quad (5)$$

where τ is used for imaginary time to be distinguished from real time t . $\mathbf{r}_{T(P)}^{\Im}$ and $\mathbf{p}_{T(P)}^{\Im}$ are position and momentum of the target (the projectile) during the tunnel-

ing process respectively. Adding the collective force corresponds to inverting the potential barrier which becomes attractive in the imaginary times. The penetrability of the barrier is given by [14]

$$\Pi(E) = (1 + \exp(2\mathcal{A}(E)/\hbar))^{-1}, \quad (6)$$

where the action integral $\mathcal{A}(E)$ is

$$\mathcal{A}(E) = \int_{r_b}^{r_a} \mathbf{P}^{coll} d\mathbf{R}^{coll}, \quad (7)$$

r_a and r_b are the classical turning points. The internal classical turning point r_b is determined using the sum of the radii of the target and projectile nuclei. Similarly from the simulation without electron, we obtain the penetrability of the bare Coulomb barrier $\Pi_0(E)$.

Since nuclear reaction occurs with small impact parameters on the atomic scale, we consider only head on collisions. The enhancement factor is thus given by eq.(1),

$$f_e = \Pi(E)/\Pi_0(E) \quad (8)$$

for each event in our simulation. Thus we have an ensemble of f_e values at each incident energy.

In Fig. 1, the upper panel shows the incident energy dependence of the enhancement factor for the D+d reaction. The averaged enhancement factors \bar{f}_e over events

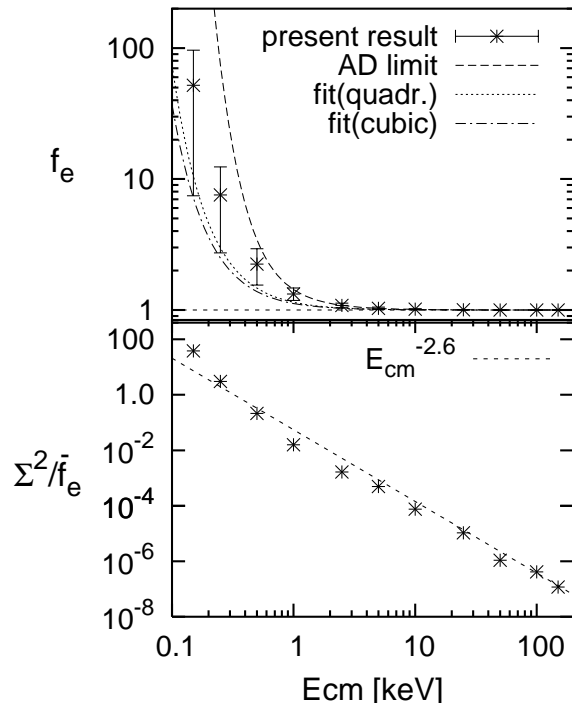


FIG. 1: Enhancement factor as a function of incident center-of-mass energy for the D+d reaction (upper panel). The corresponding Σ^2/\bar{f}_e (stars) and a power law fit (dashed line) (lower panel).

in our simulation are shown with stars and its variance $\Sigma = (f_e^2 - \langle f_e \rangle^2)^{1/2}$ with error bars. In the figure we show also several estimations of the enhancement factor by the latest analysis of the experimental data using quadratic(dotted) and cubic(dot-dashed) polynomial fitting [3] with the screening potentials $U_e = 8.7$ eV and 7.3 eV respectively. The dashed curve shows the enhancement factor in the adiabatic limit $f_e^{(AD)}$ for an atomic deuterium target and it is obtained by assuming equally weighted linear combination of the lowest-energy gerade and ungerade wave function for the electron, reflecting the symmetry in the D+d, i.e.,

$$f_e^{(AD)} = \frac{1}{2} \left(\exp(\pi\eta(E) \frac{U_e^{(g)}}{E}) + \exp(\pi\eta(E) \frac{U_e^{(u)}}{E}) \right),$$

where $U_e^{(g)} = 40.7$ eV and $U_e^{(u)} = 0.0$ eV [6, 7]. In the low energy region the enhancement factor is more than 50. However the averaged enhancement factor does not exceed the adiabatic limit. We performed also a fit of our data using eq. (2) and obtained $U_e = 15.9 \pm 2.0$ eV. This value, between the sudden and the adiabatic limit, is in good agreement with TDHF calculations[6, 7].

The ratio Σ^2/\bar{f}_e versus incident energy is plotted in the lower panel of Fig. 1. The numerical results(stars) display a self similar behavior which is well fitted by a power law with exponent -2.6 . In the high energy limit the ratio approaches zero, i.e., the f_e distribution becomes a δ -function ($\Sigma = 0$) and $\bar{f}_e \rightarrow 1$: no effects due to the electronic motion. In the low energy limit $\Sigma^2/\bar{f}_e \gg 1$, which implies a very sensitive dependence of the dynamics on the initial conditions, i.e., occurrence of chaos. Thus it is the motion of the electron which sensitively couples to the relative motion of the ions.

Similar to the gravitational 3-body problem, we look at the oscillational motions of the particle's coordinates as the projection on the z -axis (the reaction axis). We denote the z -component of $\mathbf{r}_T, \mathbf{r}_P$ and \mathbf{r}_e as z_T, z_P and z_e , respectively. Practically, we examine the oscillational motion of the electron around the target $z_{Te} = z_e - z_T$ and the oscillational motion of the inter-nuclear motion, i.e., the motion between the target and the projectile, $z_s = z_T + z_P$, which essentially would be zero due to the symmetry of the system, if there were no perturbations. In Fig. 2 these two values are shown for 2 events, which have the enhancement factor $f_e = 170.8$ (ev. A), and $f_e = 6.5$ (ev. B), at the incident energy $E_{cm} = 0.15$ keV. The panels show the z_s, z_{Te} as a function of time. The stars indicate the time at which the system reaches the classical turning point. It is clear that in the case of ev. B the orbit of the electron is much distorted from the unperturbed one than in ev. A. Characteristics of z_s are that (1) its value often becomes zero, as it is expected in the un-perturbed system, and (2) the component of the deviation from zero shows periodical behavior. It is remarkable that the amplitude of the deviation becomes quite large at some points in the case of ev. B which shows the small enhancement factor. Note that in event B one observes clear beats, i.e., resonances. Thus for two events, with the same macroscopic initial conditions, we have a

completely different outcome, which is a definite proof of chaos in our 3-body system. We can understand these results in first approximation by considering the motion of the ions to be much slower than the rapidly oscillating motion of the electrons. Thus we can consider the electron acting as an external force $F_e = F_0 \cos(\omega_H t + \delta)$, where F_0 is the amplitude of the force and ω_H is the (hydrogen) frequency. This will induce [15] a perturbation on $z_s \sim F_e/\mu\omega_H^2$, where μ is the ions reduced masses. Notice how the amplitude of z_s is actually reduced from the amplitude of z_{Te} of a factor $1 \sim 10^{-4}$, i.e., the ratio of the electron to the ion mass. We stress that this simple estimation is more relevant for case A. In fact the motion of the electron is not decoupled from the inter-nuclear motion and from energy conservation we can expect that when $|z_s|$ is maximum, $|z_{Te}|$ is minimum as observed in Fig.2, case B. Thus more generally, one should consider a perturbation where $F_0 \rightarrow F_0(t)$ and $\omega_H \rightarrow \omega_H(t)$. The time dependence of the perturbation leads, as it is well known, to the occurrence of chaos as for parametric resonance [15]. From the Fig.2 we can deduce the following important fact. If the motion of the electron is initially in the plane perpendicular to the reaction axis, the enhancement factor is large, case A(notice $|z_{Te}| \ll R_B$, i.e., the Bohr radius, at $t \sim 0$). On the other hand if there is a substantial projection of the electron motion, as in case B(the amplitude of $|z_{Te}| \sim R_B$ at $t \sim 0$), on the reaction axis the enhancement factor is relatively small because of the increase of chaoticity. This suggests that if one performs experiments at very low bombarding energies with *polarized targets*, the enhancement factor can be controlled by changing the *polarization*. The largest enhancement with targets polarized perpendicularly to the beam direction. We notice in passing that event A is a case where cylindrical symmetry is approximately satisfied, because the electron motion is practically on the xy -plane. This case gives a $U_e = 19.5$ eV closest to the adiabatic limit and to the TDHF result[6, 7].

In Fig. 3 we show the maximum amplitude of z_s for 200 events as a function of the enhancement factor f_e at the incident energy $E_{cm} = 0.15$ keV. Here we observe an evident correlation between the two values: the events which give relatively large enhancement factors correspond to the small maximum amplitude of z_s , and to the contrary, the events with relatively small enhancement factors indicate large maximum amplitudes. Since the motion of the ions is coupled to that of the electrons, it implies that an amount of energy is transferred from the relative motion of the ions to the electron thus reducing the probability of fusion. On the contrary small amplitudes imply that the electronic configuration is closer to the one in the g.s. of the compound system. Thus the binding energy of the electron is converted into the relative energy of the ions increasing the fusion probabilities.

In conclusion, we discussed the penetrability of the Coulomb barrier by using molecular dynamics simulations with constraints and imaginary time. We have shown that both the enhancement factor and its vari-

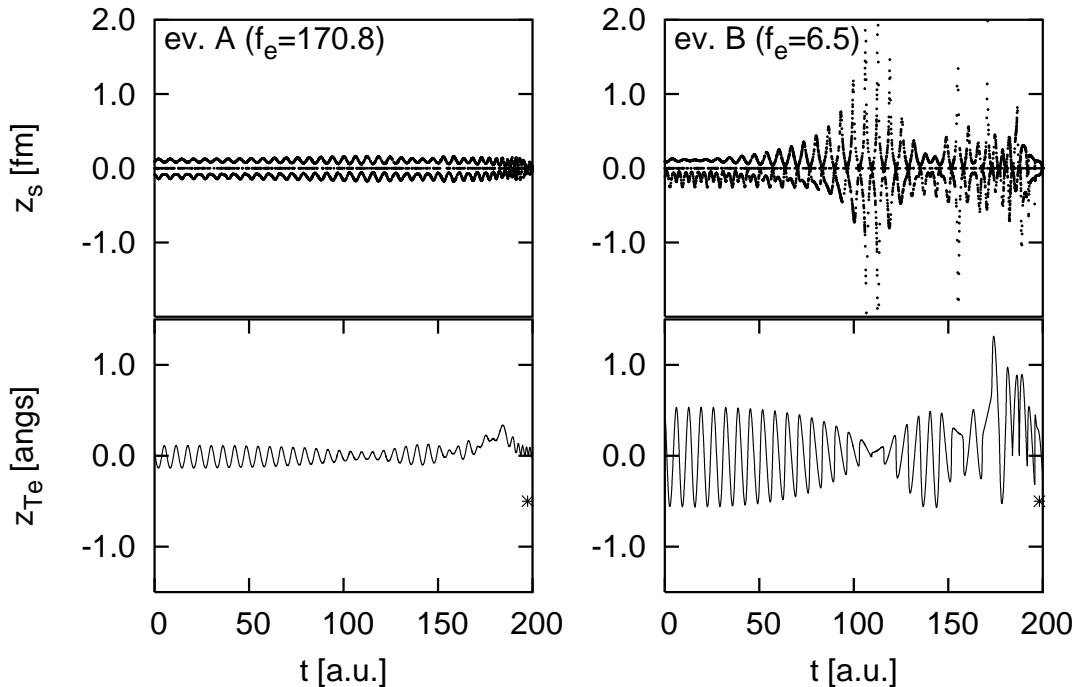


FIG. 2: The oscillational motion of the electron around the target (lower panels) and the inter-nuclear motion (upper panels) as a function of time, in atomic unit, for two events, with large f_e (ev. A) and small f_e (ev. B), for the D+d reaction at the incident energy 0.15keV. The inter-nuclear separation is 10\AA at $t = 0$.

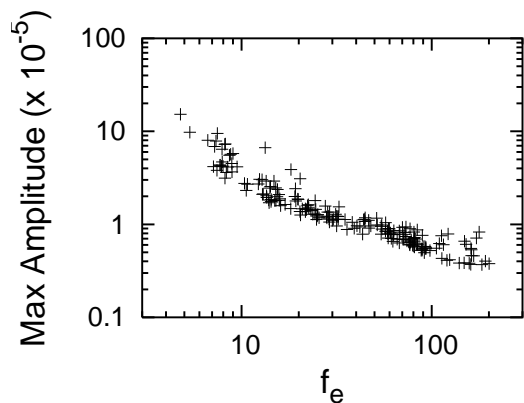


FIG. 3: The maximum amplitude of z_s for 200 events as a function of the enhancement factor f_e for the D+d reaction at the incident energy 0.15 keV.

ance increase as the incident energy becomes lower. However we obtained the averaged screening potential smaller than the value in the adiabatic limit, while from fluctuations some events clearly exceed such a limit. We pointed out that there is an evident correlation between the oscillational motion of the inter-nuclear separation and the magnitude of the enhancement factor of the cross section. The chaoticity of the electron motion affects the enhancement factor of the cross section. We suggest to perform experiments on fusion at very low energies with polarized targets.

We acknowledge valuable discussions and suggestions with Profs. D.M. Brink, G. Fiorentini, C. Rolfs, C. Spitaleri and N. Takigawa.

-
- [1] A. Krauss, *et al.*, Nucl. Phys. A **467**, 273(1987), S. Engstler *et al.*, Phys. Lett. B **202**, 179 (1988).
 [2] C. Rolfs, and E. Somorjai, Nucl. Instrum. Meth. B **99**, 297 (1995).
 [3] F. C. Barker, Nucl. Phys. A **707**, 277 (2002).
 [4] M. Junker, *et al.* Phys. Rev. C **57**, 2700 (1998).
 [5] A. Musumarra, *et al.* Phys. Rev. C **64**, 068801 (2001).
 [6] T. D. Shoppa, S. E. Koonin, K. Langanke, and R. Seki, Phys. Rev. C **48**, 837 (1993).
 [7] S. Kimura, N. Takigawa, M. Abe, and D.M. Brink, Phys. Rev. C **67**, 022801(R) (2003).
 [8] M. Papa, T. Maruyama, and A. Bonasera, Phys. Rev. C **64**, 024612 (2001), S. Terranova, and A. Bonasera, Phys. Rev. C **70**, 024906 (2004).
 [9] H. G. Schuster, *Deterministic Chaos* (VCH, Weinheim, Germany, 1995) Chap. 7, M.C. Gutzwiller, *Chaos in*

- Classical and Quantum Mechanics* (Springer Verlag, Berlin).
- [10] H. J. Assenbaum, and K. Langanke and C. Rolfs, Z. Phys. A **327**, 461(1987).
- [11] D. D. Clayton, *Principles of Stellar Evolution and Nucleosynthesis* (University of Chicago Press, 1983) Chap. 4.
- [12] J.A. Bearden, and A.F. Burr, Rev. Mod. Phys, **39**, 125(1967).
- [13] S. Kimura, and A. Bonasera, physics/0409008.
- [14] A. Bonasera, and V. N. Kondratyev, Phys. Lett. B **339**, 207(1994), T. Maruyama, A. Bonasera, and S. Chiba, Phys. Rev. C **63**, 057601(2001).
- [15] L. D. Landau, and E. M. Lifshitz, *Mechanics* (Pergamon Press, 1976) Chap. 5.